

Spectrum Occupancy Measurements and Analysis Methods on the 2.45 GHz ISM Band

Joonas Kokkonen and Janne Lehtomäki
Centre for Wireless Communications (CWC)
University of Oulu, Finland
Email: joonas.kokkonen@ee.oulu.fi, jannel@ee.oulu.fi

Abstract—We performed spectrum occupancy measurements on the 2.45 GHz Industrial, Scientific and Medical (ISM) band in the area of Oulu, Finland. The comprehensive measurement campaign consisted of eight different locations and ten different measurement occasions, each with approximately one week of continuous spectrum monitoring. The measurement data is analyzed from the viewpoint of fitting new systems on 2.45 GHz ISM band, rather than pure duty cycle analysis. To aid accurate analysis, we propose Transmission Encapsulation based on the Connected Component Labeling (TECCL). This novel method searches for the clusters of connected signal components in the time-frequency grid and provides the extreme dimensions of each cluster for the subsequent analysis. It is shown that the TECCL does not cause a significant increase in the false alarm probability. Our results indicate that new systems with cognitive radio capabilities could be introduced to 2.45 GHz ISM band.

I. INTRODUCTION

Current inflexible radio resource allocation will exhaust available radio frequencies. Several measurements have shown that the spectrum is sparsely utilized both on licensed and unlicensed frequency bands [1]–[9]. A possible solution for this problem is cognitive radios (CRs) that can utilize radio frequency spectrum without needing fixed allocations. This approach is based on using the spectrum only when it is not being used by the primary user or other co-existing users.

One of the most interesting unlicensed frequency bands is the globally available 2.45 GHz industrial, scientific and medical (ISM) band. This band is used by, e.g., wireless local area network (WLAN), Bluetooth, and ZigBee devices. The 2.45 GHz ISM band is interesting due to flexible spectrum access, thus CRs could operate on the band by avoiding the coexisting systems. Due to potentiality of 2.45 GHz ISM band, many CR test beds have been developed for this band, e.g. [10] and [11, Ch. 4.2.4]. Some unlicensed devices on the ISM band already access the spectrum intelligently. For example, Bluetooth devices can withdraw from the frequencies utilized by the other devices [12].

Spectrum occupancy measurements in the 2.45 GHz ISM band are needed in order to see if there is still space for intelligent CR systems. Due to vast amount different kinds of devices and applications allocated to this band, local differences in the spectrum utilization may be significant. This is also enhanced by the low transmission powers. Therefore

This research was funded by the Finnish Funding Agency for Technology and Innovation (TEKES).

the radio environment may vary significantly even inside a small area and spectrum occupancy measurements should be conducted in several locations. The majority of the previous spectrum surveys have been focusing on wide-band measurements, usually with a generic monitoring device not optimized for ISM band measurements. Also, many of the previous measurement campaigns have been conducted in large cities, such as Barcelona [1], Chicago [3] and Tokyo [5]. In the previous measurement campaigns, the duty cycles on 2.45 GHz ISM band have generally been observed to vary between approximately 0 and 15 %. Some higher utilizations have been measured, but the occupancies have usually been low.

In this paper, we provide the results of a measurement campaign on 2.45 GHz ISM band conducted in eight different locations, with the total of ten measurements in the area of Oulu and in the neighboring municipalities of Oulu. Each of the measurement occasions lasted for approximately one week. Since the city of Oulu is one of the biggest cities in Finland, these measurements also give typical utilization values for a Finnish city. However, Finnish cities are relatively small in comparison with the major cities globally. The analysis of the measurement results focuses on the suitability of this band for possible new systems regarding aspects such as the number of available channels. A new analysis method called transmission encapsulation based on the connected component labeling (TECCL) is proposed. This novel method searches for the clusters of connected signal components in the time-frequency grid and provides the extreme dimensions of each cluster for the subsequent analysis.

The rest of this paper is organized as follows. Section II presents the measurement setups and the measurement locations. Section III provides information on the analysis methods and most importantly, introduces the TECCL. Section IV gives the results of this measurement campaign and finally, Section V concludes this paper.

II. MEASUREMENT SETUP

A. Measurement Equipment

The main measurement equipment was Fluke Networks PC Card Sensor mounted into IBM ThinkPad T42 PCMCIA slot. This sensor is capable of monitoring both WLAN bands, 2.4–2.5 GHz ISM band, and 4.94–5.85 GHz band (partially ISM band). This device directly calculates the duty cycle for each frequency bin by calculating the fraction of the fast Fourier

transforms (FFTs) exceeding the threshold (γ) of 20 dB above the noise floor according to

$$DC_j = \frac{100}{N} \times \sum_i^N X_{ji}, \quad (1)$$

where DC_j is the duty cycle of the j th frequency bin (in percents), N is the number of FFTs per time interval over which the duty cycle is calculated and X_{ji} is

$$X_{ji} = \begin{cases} 1 & \text{if } |x_{ji}|^2 > \gamma \\ 0 & \text{else} \end{cases} \quad (2)$$

where x_{ji} is the sample of the j th frequency bin produced by the FFT and γ is the threshold. Fluke PC Card divides the monitored spectrum into 20 MHz dwells. At least 200 FFTs are done for each dwell per second. The frequency bin separation of this device is 156 kHz, thus there are 641 frequency bins on the 2.45 GHz ISM band. The PC Card Sensor calculates the raw data matrix based on these parameters and according to (1). The time interval over which the duty cycle (for the whole 2.45 GHz band) is calculated, is one second [13]. The noise floor of the sensor was tested in the electromagnetic compatibility (EMC) laboratory (anechoic chamber) of the University of Oulu. The measurements resulted in a mean average power of -116.86 dBm (measured over all of the samples during the time period of 12 minutes and 55 seconds). Therefore the sensitivity for the duty cycle measurements was approximately -96 dBm per 156 kHz sub-bands due to 20 dB threshold. Visualization of the Fluke PC Card data was done with the Fluke Networks AnalyzeAir Wi-Fi Spectrum Analyzer 3.0 software. This software was also used to export the data into Excel files with AutoIT script¹. The data in these Excel files was extracted and further processed with MATLAB software. Fig. 1 depicts the measurement equipment and the processing flow of the measurement data.

One additional comparative measurements were performed in order to compare the results given by the different measurement system and configuration. The main equipment of this setup was Agilent N6841A RF sensor. The input to the sensor was filtered with Creowave ISM band filter and amplified with Mini-Circuits ZRL-3500 low noise amplifier (LNA). The RF sensors output had 916 frequency bins (in comparison with Flukes 641), giving the frequency bin separation of 109.375 kHz. Due to the shape factor utilized for sideband level performance improvement, the resolution bandwidth (RBW) was 242.27 kHz. The frequency bin revisit time was approximately ten milliseconds and the sensitivity of the measurement system was approximately -100 dBm. The raw data matrix for this setup was calculated by taking the average over approximately two seconds according to equation (1). This measurement setup has been used, for instance, in [14] and [15].

B. Measurement Locations

Measurement campaign locations included Sokos Hotel Arina and the premises of Sensinode Ltd. in the center of Oulu,

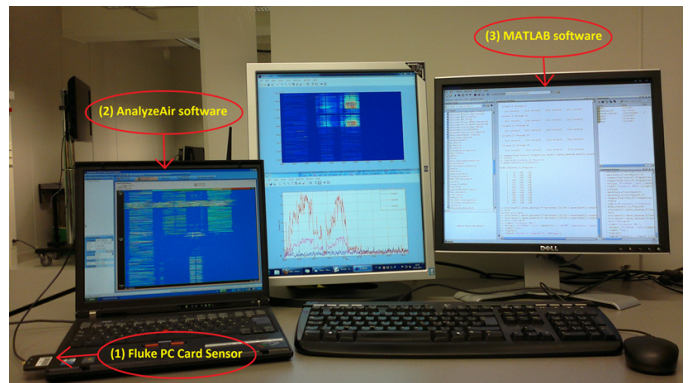


Fig. 1. Measurement equipment and the processing flow of the measurement data.

the residential area of Toppila in the western part of Oulu, a rural area location in Haukipudas and three campus area locations in the premises of University of Oulu. In addition, Oulu Airport was monitored with the additional measurement equipment presented previously.

The three campus area locations were divided into office measurement at the Centre for Wireless Communications (CWC), Tellus library and conference measurements during 37th Euromicro Conference on Software Engineering and Advanced Applications (SEAA 2011) and 14th Euromicro Conference on Digital System Design (DSD 2011). The measurements in Tellus library and Toppila were bipartite and the aim was to study the differences between two independent measurement occasions. The first measurements in Tellus library were conducted during the summertime when only a few students were presents. The second measurements were conducted during the autumn term when the library was fully utilized. The measurements in Toppila were performed twice approximately two months apart from each other. This way the difference in the utilization could be evaluated between two uncorrelated time periods in the same measurement spot.

The shortest measurements were conducted in the rural area location (approximately 5 days of continuous measurements) while the rest of the locations were monitored for approximately from 7 to 8 days.

III. ANALYSIS METHODS

Since the measurement equipment were producing the raw data matrix Ω_{ij}^d , where i is the time interval index and j is the frequency bin index, the measurement data was used “as is” for separate time and frequency domain utilization analysis. However, since the new system candidates require bandwidth, available bandwidth analysis was done via TECCL. This is due to need for a hard decision whether the signal exists in a certain time-frequency element or not. This could be achieved by just thresholding the measurement data, but the TECCL was used to provide guard areas around the extreme dimensions of the detected transmissions, thus giving somewhat more pessimistic image of the spectrum usage.

¹<http://www.autoitscript.com/site/>

A. TECCL

The most important analysis method was the proposed TECCL. In this novel method, the nearby transmissions are encapsulated in order to fill the signal space around the transmission clusters. This is due to the attenuation of the signals on the radio channel. Especially in the frequency domain, strongly attenuated signals usually appear to be narrower than they are in reality. This method fills the gaps between the signals both in frequency and time domains, provided that transmissions are close enough to each other. TECCL is based on connected component labeling (CCL) [16]. CCL is one of the algorithms used in the graph theory and is used, for instance, in the machine vision applications. CCL groups, for example, the pixels of the photograph. The pixels are given labels based on the values of the pixels and the position of the pixels relative to the other pixels. This is explained in detail in [16].

The transmission encapsulation method presented here is a three-phase process for the duty cycle data:

- 1) Thresholding the elements (Ω_{ij}^d) of the raw measurement data matrix Ω^d with the threshold level λ to produce the binary data matrix Ω^b (of the binary elements Ω_{ij}^b).

$$\Omega_{ij}^b = \begin{cases} 1 & \text{if } \Omega_{ij}^d > \lambda \\ 0 & \text{else} \end{cases} \quad (3)$$

- 2) Connected component labeling for the Ω^b .
- 3) Encapsulation of the transmission clusters based on the extreme dimensions of individually labeled clusters in order to produce the TECCL binary data matrix Ω_{TECCL} .

Fig. 2 depicts the processing flow of the transmission encapsulation. In Fig. 2 (a) is the original measurement data Ω^d and the rest of the figures depicts the situation after each of the phases described above. The figures depict a small portion of an actual measurement data, with 101 frequency bins and 31 seconds.

The aim of the phase one is to form a binary matrix Ω^b from the Ω^d (i.e. ‘1’ for occupied and ‘0’ for unoccupied). In the analysis of this paper, a fixed threshold $\lambda = 5\%$ for the measured duty cycle data was used in order to reject less important transmissions, such as beacon signals. Similar decision should also be made by the CR (on 2.45 GHz ISM band), since, for instance, Bluetooth is using all the channels if the spectrum contains no other transmissions. Therefore the decision of which signals can be overlapped with must be made by the CR. In this case, this is done by adjusting the threshold level. However, the fact that some frequencies are used by some co-existing system, does not mean that the very same frequencies could not be used by the secondary systems. If the co-existing system is causing, for instance, 10% occupancy on some frequency band, this directly means that the band is available 90% of the time. These unoccupied time instants could be utilized by the secondary systems, provided that the secondary system can avoid the time instants utilized by the primary system (time agile CR, e.g. [17]). Fig. 2 (b) depicts the binary duty cycle Ω^b after the thresholding.

The second phase is the most important part of this analysis method. CCL is used to identify and isolate the individual transmission clusters from Ω^b , i.e. transmissions, which are connected to each other in the time-frequency grid within the limits of time domain resolution and resolution bandwidth. CCL groups the connected “pixels” (in this case, the connected time-frequency elements exceeding the threshold) and gives each group an individual label, i.e. a sequential number, that can be used to determine the coordinates of all of the individual pixels in the group by extracting only those elements from the data matrix with a certain label. From the viewpoint of the TECCL, this is the method for capturing the coordinates and therefore the positions of the transmission clusters.

The third phase is to find the extreme dimensions of each cluster carrying a unique label. Based on the maximum and minimum position values in the time and frequency domains, all the matrix elements within the rectangles are given a value of ‘1’ to indicate the occupied time instants and the frequency bins. The given rectangle shape for the transmission clusters is also practical since the real-life signals are rectangles in an ideal case. Fig. 2 (d) shows the TECCL outcome matrix Ω_{TECCL} . From (d) it can be seen how the frequency and time domain gaps of the different clusters have been filled.

By performing the procedure above, the detected connected transmissions are unified in order to decrease the number of the short time and frequency domain gaps caused by the attenuation of the signals in the radio path. The danger behind the TECCL is extensive overestimation in the case that two transmissions are cutting each other. On the other hand, CR should avoid utilized frequencies, thus this overestimation may be a positive occurrence. The phase one of the TECCL could be enhanced with, for instance, the localization algorithm based on double thresholding (LAD) methods. This would give a better performance in the case of the low signal-to-noise ratio (SNR) signals, since the attenuation lowers the duty cycle due to transmissions invisible to the measurement equipment. The LAD is introduced in [18].

The binary data matrices produced by TECCL were used to calculate the bandwidth aggregation values. The bandwidth aggregation tells the total amount of free spectrum per time interval over which the duty cycle is calculated

$$B_i = \Delta_f \times \sum_{j=1}^M \Omega_{ij}^{TECCL}, \quad (4)$$

where B_i is the bandwidth aggregation for the i th time instant, Δ_f is the frequency resolution of the data matrix, M is the number of the frequency elements per time instant and Ω_{ij}^{TECCL} are the time-frequency elements of Ω_{TECCL} . TECCL was also used in the calculation of the number of free channels per time instant. This statistic was achieved by calculating the width of each whitespace in the frequency domain per time instant and calculating the number of channels fitting into the spectrum openings with respect to the bandwidth of

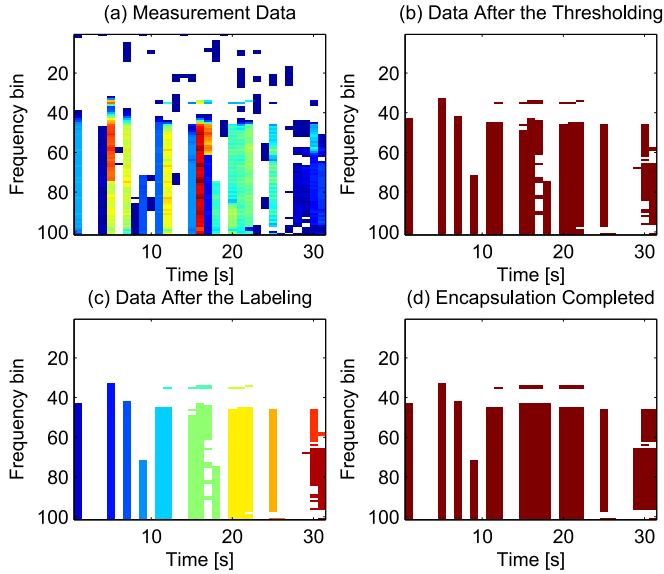


Fig. 2. Processing flow of the TECCL.

the channel

$$N_{i,B} = \sum_{B_i^{SO}} \lfloor \frac{B_{ik}^{SO}}{B_{ch}} \rfloor, \quad (5)$$

where $N_{i,B}$ is the number of available channels utilizing the bandwidth B for the i th time instant, $\sum_{B_i^{SO}}$ is the sum over all the spectrum openings of the vector B_i^{SO} of the i th time instant. The B_i^{SO} is a collection of the bandwidths of the contiguous groups of zeros for the time interval i . $\lfloor \frac{B_{ik}^{SO}}{B_{ch}} \rfloor$ is the integer part of the division between the bandwidth of the k th spectrum opening B_{ik}^{SO} and the bandwidth of the desired channel B_{ch} . For example, we can fit 2 20 MHz channels into a contiguous opening of 42 MHz. This paper presents the number of available channels per time interval for five different bandwidths: 20, 40, 60, 80 and 100 MHz.

B. False alarm performance of TECCL

TECCL may increase the effect of false alarms if the samples exceeding the threshold are close to each other, i.e. TECCL forms a guard area around a cluster of false alarms, thus increasing the number of erroneously detected signals in the adjacent time-frequency elements. The TECCL false alarm performance was tested by simulations with MATLAB. Fig. 3 illustrates the results of the simulations. At the first stage, random 500×500 binary matrices were produced with the certain probabilities for '1'. These random matrices illustrated the empty measurement data matrices and ones were representing the false alarms. The probability of value '1' (Bernoulli distribution parameter p) was corresponding the probability of false alarm (PFA). For each Bernoulli distribution parameter p , separate element-wise PFAs, i.e. the fraction of the number of ones with respect to the number of elements in the data matrix, were calculated for the random binary matrices (representing the outcome of the phase one in the TECCL) and for the TECCL processed binary matrices.

The blue and red lines in Fig. 3 depicts the simulated element-wise PFA values as a function of Bernoulli's PFA for the random binary matrices and the TECCL, respectively. It can be seen from the figure that TECCL increases the element-wise PFA by approximately 0.04, 0.16 and 0.38 percentage points compared with the unprocessed PFA values of 1, 2 and 3 % respectively. Therefore the effect of the TECCL on the PFA can be considered minor.

Theoretical values for TECCL were calculated for the PFA values ranging from 0% to 3%. The false alarms in different time-frequency elements were assumed to be independently and identically distributed (i.i.d.), i.e. the pattern of (or the number of) false alarms for a specific PFA can not be predicted. Therefore, for each PFA, all the possible combinations of the binary matrices with sizes of 3×3 and 5×5 were went through (512 combinations for the 3×3 matrix and 33,554,432 combinations for the 5×5 matrix). If '1' represents the false alarm, by evaluating the center element of the 'binary data matrix' Ω^b before and after the TECCL and by weighting the value with the probability of the Ω^b with respect the PFA at issue, the output shows the theoretical effect of the TECCL on the PFA. Weighting factor w for the probability of Ω^b is calculated with equation

$$w = \text{PFA}^{\sum_i \sum_j \Omega_{ij}^b} \times (1 - \text{PFA})^{n^2 - \sum_i \sum_j \Omega_{ij}^b}, \quad (6)$$

where $\sum_i \sum_j \Omega_{ij}^b$ is the number ones in the Ω^b and n is the dimension of the square matrix. Weighting is done in order to take into consideration the probability of the certain false alarm matrix, for instance, it is improbable that all the elements of Ω^b are ones if PFA is 1%. The evaluation of the center element of the 3×3 matrix tells the effect of the TECCL on the adjacent elements to the single matrix element. 5×5 matrix tells the same and in addition the effect of the TECCL on the next closest element in the matrix. Due to the fact that 3×3 already produced accurate results, the element-wise PFA increase of the TECCL is mainly caused by the adjacent time-frequency elements. This is due to typically low PFA values, i.e. if the element-wise PFA is low, it is unlikely that the false alarms would form large uniform clusters.

IV. RESULTS

Table I summarizes the key results of this measurement campaign. The highest mean duty cycle was recorded at Oulu Airport, the second busiest airport in Finland, with 3.19% average utilization. This is due to the three strong WLAN signals at the airport of which one was constantly causing approximately 8.7 % occupancy. This high continuous utilization was not met elsewhere and therefore this signal was assumed to belong to the airports internal data transferring. This location was monitored with the additional measurement setup, which was somewhat more sensitive. On the other hand, in the test measurements the differences between the two setups were minor, thus higher average spectrum utilizations were most likely caused by the location itself with higher number of users than in the other locations.

TABLE I
MEAN NUMBER OF AVAILABLE CHANNELS AND MEAN BANDWIDTH AGGREGATION

Location	Mean Duty Cycle [%]	Busy Hour Mean [%]	Number of Channels per [MHz] ch. (Busy Hour)					Mean Bandwidth Aggreg. [MHz]	BH Bandwidth Aggreg. [MHz]
			20	40	60	80	100		
Sokos Hotel Arina	0.30	12.6	4.91 (2.84)	1.96 (1.01)	0.97 (0.02)	0.96 (0.01)	0.94 (0.01)	99.45	76.78
Sensinode Ltd.	0.47	1.1	4.17 (3.58)	1.72 (1.46)	0.96 (0.94)	0.71 (0.45)	0.43 (0.12)	94.95	88.82
Toppila P1	1.05	8.9	3.45 (2.15)	1.03 (0.02)	0.32 (6e-4)	0.20 (3e-4)	0.20 (3e-4)	87.52	70.81
Toppila P2	1.16	4.0	3.32 (2.84)	1.15 (0.96)	0.50 (0.42)	0.32 (0.15)	0.20 (0.09)	86.42	83.07
Haukipudas	4.5×10^{-5}	n/a	~ 5 (n/a)	~ 2 (n/a)	~ 1 (n/a)	~ 1 (n/a)	~ 1 (n/a)	~ 100	n/a
CWC	0.69	1.7	4.47 (3.53)	1.75 (1.36)	0.80 (0.59)	0.70 (0.36)	0.66 (0.19)	97.00	87.78
Tellus library P1	0.62	1.8	4.40 (4.15)	1.98 (1.77)	0.97 (1.00)	0.96 (0.77)	0.43 (0.38)	94.00	91.91
Tellus library P2	0.91	4.8	4.21 (3.03)	1.87 (1.02)	0.87 (0.98)	0.83 (0.02)	0.34 (0.01)	92.90	82.97
SEAA & DSD	0.42	3.4	4.84 (3.86)	1.88 (1.35)	0.96 (0.50)	0.88 (0.36)	0.88 (0.36)	98.68	90.78
Airport of Oulu	3.19	8.5	2.38 (1.98)	0.57 (0)	0.18 (0)	0.15 (0)	$3e-4$ (0)	68.8	65.08

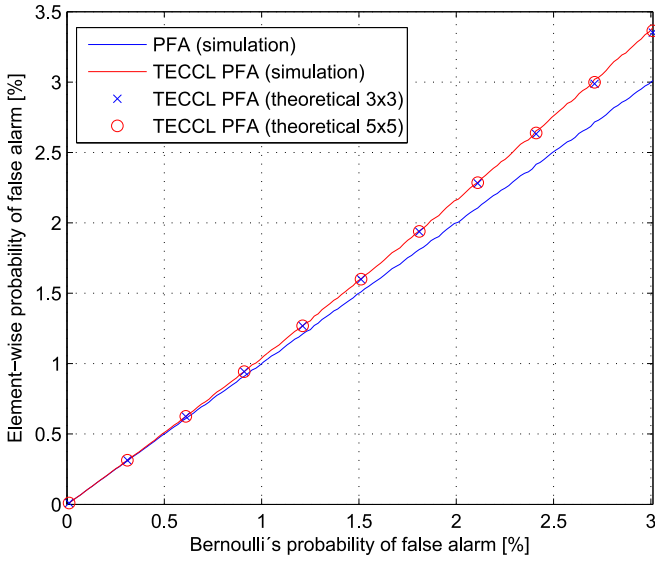


Fig. 3. The false alarm increase caused by TECCL.

Other locations produced much lower values, with the lowest utilizations in the rural area of Haukipudas. The spectrum was almost entirely deserted in this location. The mean duty cycles were calculated over the entire week from 100 MHz bandwidth. This decreases the mean values since during the nighttimes, the spectrum is usually more or less idle.

The busy hour statistics were produced due to need for an information on the worse-case scenario occupancies. These values were calculated by searching the most utilized hour of each location (except for Haukipudas, where the spectrum was virtually free all the time). There were very little trends how the busy hours were distributed. Sensinode Ltd. and the campus locations, for instance, produced the highest utiliza-

tions during the daytime due to opening hours. However, what seemed to matter, was the random time instant when a single user initialized high data rate traffic, such as downloading a large file or streaming a video. Values presented in Table I are the average values over 100 MHz bandwidth during the most occupied hour. It can be seen that the second least utilized location, Sokos Hotel Arina, produced the highest busy hour occupancy. This was caused by a single WLAN channel, on which the utilization increased up to 100% for a three-hour time period. Interestingly, the airport did not produce very high busy hour utilization although the mean duty cycle was the highest. This is partially caused by the airports even spectrum utilization both in time, and frequency domains.

The two bipartite measurements resulted in interesting findings. The measurements in Tellus library of the University of Oulu showed what was expected: during the first measurements the difference between the nighttimes and the daytimes was moderate due to a few visitors during the summertime. The second measurements resulted in much higher occupancies, thus higher differences. Fig. 4 depicts the mean time domain occupancies measured on the WLAN channel 1 (center frequency 2412 MHz) and on 2.45 GHz ISM band. While the nighttime usages had stayed the same, the daytime utilizations had multiplied since the first measurements. However, since the library is closed during the nighttimes, the mean occupancies did not increase significantly.

The both measurements in Toppila resulted in similar utilizations. However, the frequency allocation of the WLAN base stations had changed between the two monitoring periods. Fig. 5 depicts the mean frequency domain utilizations during the both measurements. The figure clearly shows how the two strong WLAN signals on the channels 11 and 12 (center frequencies 2462 MHz and 2467 MHz) had moved to the channels 1 (2412 MHz) and 10 (2457 MHz) respectively. This

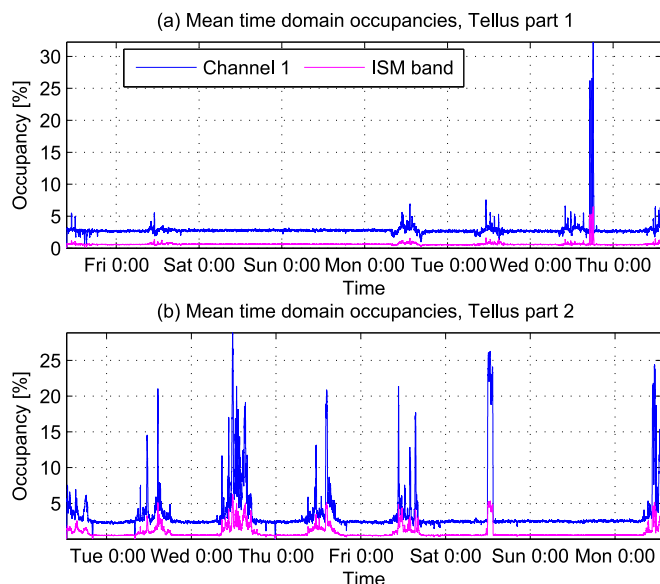


Fig. 4. The mean time domain occupancies in Tellus library.

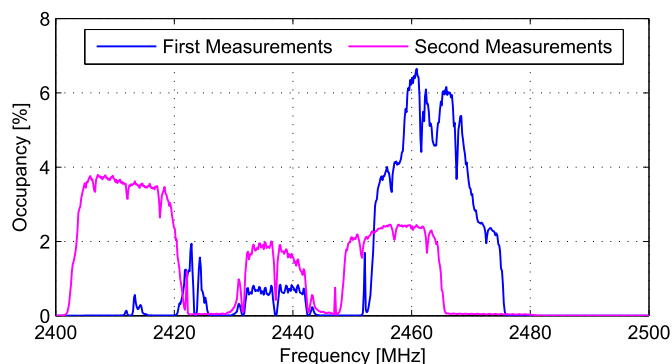


Fig. 5. The mean frequency domain occupancies in Toppila.

shows that spectral situation may change significantly even within a relatively short period of time. The minor increase in the overall utilization in this location was due to the higher occupancies on the WLAN channel 6 (2437 MHz).

Low utilizations can also be seen in the channel availability statistics. If we consider a new system with the bandwidth of 20 MHz, each of the locations could have, on average, several parallel channels without causing interference to the existing systems. Only during the busy hours the CR would have to cope with fewer channels. The last two columns of the Table I presents the bandwidth aggregation values for both, the whole measurement time period and the busy hour (BH). These values also show how unutilized the spectrum was. The airport produced significantly lower mean available bandwidths. This is partly due to the higher occupancies, but also due to the measurement equipment. The Agilent RF Sensor did have less time domain gaps with comparison to the Fluke Networks PC Card Sensor. This is directly effecting on the available bandwidths. However, mean available bandwidth 68.8 MHz can still be considered very high.

V. CONCLUSION

Based on this occupancy measurement campaign, there is no reason why cognitive radios could not operate on 2.45 GHz ISM band in the area of Oulu. On the contrary, CR using, for instance, 20 MHz of bandwidth could use the band without causing harmful interference to the existing systems. The occupancies were very low in all of the measurement location with the mean occupancies ranging between approximately 0 and 3%. Also, very wide bandwidths were available in all of the locations, even during the busy hours. These are very encouraging result with respect to the CRs. The downside of 2.45 GHz ISM band is the transmit power regulations, which often limits the theoretical cell sizes to be relatively small. However, this band can still be kept as a interesting opportunity for the CRs.

REFERENCES

- [1] M. López-Benítez and F. Casadevall, "On the spectrum occupancy perception of cognitive radio terminals in realistic scenarios," in *Proc. CIP*, 2010.
- [2] M. H. Islam, C. L. Koh, S. W. Oh, X. Qing, Y. Y. Lai, C. Wang, Y.-C. Liang, B. E. Toh, F. Chin, G. L. Tan, and W. Toh, "Spectrum Survey in Singapore: Occupancy Measurements and Analyses," in *Proc. CROWNCOM*, 2008.
- [3] T. M. Taher, R. B. Bacchus, K. J. Zdunek, and D. A. Roberson, "Long-term Spectral Occupancy Findings in Chicago," in *Proc. DySPAN*, 2011.
- [4] M. McHenry, D. McCloskey, G. Minden, and D. Roberson, "Multi-Band, Multi-Location Spectrum Occupancy Measurements," in *Proc. ISART*, 2006.
- [5] J. Naganawa, H. Kim, S. Saruwatari, H. Onaga, and H. Morikawa, "Distributed spectrum sensing utilizing heterogeneous wireless devices and measurement equipment," in *Proc. DySPAN*, 2011.
- [6] T. Harrold, R. Cepeda, and M. Beach, "Long-term Measurements of Spectrum Occupancy Characteristics," in *Proc. DySPAN*, 2011.
- [7] K. A. Qaraqe, H. Celebi, A. Gorcin, A. El-Saigh, H. Arslan, and M. slim Alouini, "Empirical Results for Wideband Multidimensional Spectrum Usage," in *Proc. PIMRC*, 2009.
- [8] M. Biggs, A. Henley, and T. Clarkson, "Occupancy analysis of the 2.4GHz ISM band," *IEE Proceedings-Communications*, vol. 151, pp. 481-488, 2004.
- [9] L. Stabellini, "Quantifying and Modeling Spectrum Opportunities in a Real Wireless Environment," in *Proc. WCNC*, 2010.
- [10] S. M. Mishra, D. Cabric, C. Chang, D. Willkomm, B. van Schewick, A. Wolisz, and R. W. Brodersen, "A Real Time Cognitive Radio Testbed for Physical and Network level Experiments," in *Proc. DySPAN*, 2005.
- [11] M. Matinmikko and T. Bräysy, "Towards Cognitive Radio Systems, Main Findings from the COGNAC Project," VTT Technical Research Centre of Finland, Centre for Wireless Communications (University of Oulu), Tech. Rep., 2011. [Online]. Available: <http://www.vtt.fi/inf/pdf/tiedotteet/2011/T2575.pdf>
- [12] *Specification of the Bluetooth System (Bluetooth Specification Version 4.0)*, Bluetooth Special Interest Group Std.
- [13] *AnalyzeAir Wi-Fi Spectrum Analyzer 3.1: User Manual*, Fluke Networks, 2007.
- [14] J. J. Lehtomäki, J. Vartiainen, R. Vuontoniemi, and H. Saarnisaari, "Adaptive FCME-Based Threshold Setting for Energy Detectors," in *Proc. CogART*, 2011.
- [15] J. J. Lehtomäki, R. Vuontoniemi, K. Umebayashi, and J. P. Mäkelä, "Energy Detection Based Estimation of Channel Occupancy Rate With Adaptive Noise Estimation," *IEICE Transactions on Communications*, vol. E95-B, no. 04, Apr. 2012.
- [16] L. D. Stefano and A. Bulgarelli, "A Simple and Efficient Connected Components Labeling Algorithm," in *Proc. ICIAP*, 1999.
- [17] L. Biard, D. Noguét, T. Gernandt, P. Marques, and A. Gameiro, "A Hardware Demonstrator of a Cognitive Radio System Using Temporal Opportunities," in *Proc. CROWNCOM*, 2009.
- [18] J. Vartiainen, J. J. Lehtomäki, and H. Saarnisaari, "Double-Threshold Based Narrowband Signal Extraction," in *Proc. VTC*, 2005.